Performance Analysis of CNN-based Autoencoders Under Generalized Fading Channels

Pedro M. R. Pereira, Amin Hoseini, Samuel B. Ferreira Gomes, Felipe A. P. de Figueiredo, Rausley A. A. de Souza, Gustavo Freindenraich and Michel Daoud Yacoub

***Abstract*— The emergence of deep learning (DL) in wireless communications has revolutionized the design of transceivers, enabling end-to-end learning-based systems such as autoencoders. Unlike traditional communication systems that rely on separately optimized blocks for encoding, modulation, and decoding, an autoencoder jointly optimizes the transmitter and receiver, leading to potentially more efficient and adaptive communication. However, the performance of such architectures under practical fading conditions remains an open research question. This paper investigates the block error rate (BLER) performance of a convolutional neural network (CNN)-based autoencoder under a generalized fading model. Specifically, we adopt the κ-μ fading model due to its flexibility in representing various real-world fading scenarios. We also analyze classical modulation schemes' analytical BLER under the same fading conditions to establish a meaningful comparison. Through simulations, we demonstrate that the CNN-based autoencoder efficiently adapts to different fading environments while maintaining robust performance, showcasing its potential as a viable alternative to conventional communication system designs.**

***Keywords*— Deep Learning, Autoencoder, Convolutional Neural Network, Wireless Communication, Fading.**

I. Introduction

Wireless communication systems continuously evolve to meet the increasing demands for reliability, efficiency, and adaptability in diverse and challenging environments. Traditional communication architectures are based on well-defined signal processing blocks such as modulation, channel coding, and equalization, which are designed and optimized independently [1], [2]. However, these conventional systems often struggle to perform optimally under complex fading conditions.

Autoencoder-based architectures have been proposed as an alternative to traditional communication systems, leveraging DL to learn the entire transceiver process as an end-to-end optimization problem. The work in [3] introduced the concept of communication systems modeled as autoencoders, demonstrating that such systems can achieve competitive BLER performance compared to classical methods. Further extensions explored the integration of adversarial networks to enhance multi-user communication and the application of CNNs for modulation classification, achieving performance comparable to feature-engineered approaches [3].

Pedro M. R. Pereira, Felipe A. P. de Figueiredo, and Rausley A. A. de Souza are with the National Institute of Telecommunications (INATEL). Emails: {pedro.marcio, felipe.figueiredo, rausley}@inatel.br. Amin Hoseini, Samuel B. Ferreira Gomes, and Gustavo Freindenraich are with UNICAMP. Emails: amin.hosei@gmail.com, {samuelbf,gf,michel}@decom.fee.unicamp.br

DL has also been applied to wireless communication challenges, such as channel estimation and mitigation of interference. In [4], a convolutional denoising autoencoder with an attention mechanism was proposed to predict channel conditions in intelligent reflecting surface (IRS)-assisted millimeter-wave communications, showing significant improvements in signal quality and energy efficiency. Similarly, [5] investigated an autoencoder with a fitting network for Terahertz (THz) communication, demonstrating its viability to mitigate hardware imperfections and channel distortions.

Another important line of research focuses on the robustness of autoencoder-based communication systems under practical channel conditions. The work in [6] proposed a DL-based channel estimation technique for chaotic wireless communication, leveraging a stacked denoising autoencoder to improve resilience against noise. Similarly, [7] validated the feasibility of over-the-air communication using purely neural network-based transceivers, achieving competitive BLER performance against traditional schemes. Furthermore, [8] introduced a differential autoencoder design for optical wireless communication, optimizing constellation points to minimize shot noise effects and improve bit error rate (BER) performance. The performance analysis for an autoencoder under the α-μ channel was made in [9], and [10]. A CNN-based architecture was employed in [9], assuming perfect channel state information (CSI) at the receiver. In contrast, [10] extends the analysis to a more complex fading environment incorporating shadowing and mobility effects using a dense neural network (DNN)-based architecture.

Despite these advancements, a comprehensive study on the BLER performance of CNN-based autoencoders under generalized fading conditions remains an open research problem. Most prior studies have focused on specific fading models or have not evaluated autoencoder-based systems in highly dynamic channel environments. This paper addresses this gap by investigating the performance of a CNN-based autoencoder under the κ-μ fading model, which represents various real-world fading conditions. The main contributions of this paper are as follows: i) We analyze the BLER performance of a CNN-based autoencoder in κ-μ fading conditions, ii) We compare the CNN-based autoencoder's BLER performance with analytical results for classical modulation schemes under the same fading conditions, and iii) We present simulation results demonstrating that the CNN-based autoencoder efficiently adapts to different fading environments while maintaining robust communication performance.

The rest of this paper is structured as follows. Section II

reviews related work in DL-based communication systems and autoencoder architectures. Section III describes the channel model. Section IV presents performance analysis and simulation results. Finally, Section V concludes the paper.

II. Autoencoder-Based End-to-End Communication System

A conventional point-to-point communication system comprises three primary components: the transmitter, the channel, and the receiver. The transmitter conveys a message m over the channel to the receiver, where the message consists of a sequence of L symbols (block length), each symbol encoding k information bits. Consequently, the number of discrete channel uses is denoted as n, and the system's transmission rate is defined as $R = k/n$ (bits per channel use). The transmitter applies a transformation function $x = f(m) \in \mathbb{C}^n$, generating the transmitted signal x.

Transmitter hardware typically imposes constraints on x, which in this study is represented as a power constraint $||x||^2 \leq n$. The channel is modeled as a stochastic system, where the received signal follows a conditional probability function $y \sim p(y|x)$, with $y \in \mathbb{C}^n$ representing the received signal. The receiver then applies a transformation $\hat{m} = g(y)$ to estimate the original message m with minimal error. Within the DL framework, the transmitter and receiver are referred to as the encoder and decoder, respectively, and are implemented using neural networks, as depicted in Fig. 1.

A feedforward neural network establishes a mapping $f(x_0; W) : \mathbb{R}^{N_0} \to \mathbb{R}^{N_L}$ from an input vector $x_0 \in \mathbb{R}^{N_0}$ to an output $x_L \in \mathbb{R}^{N_L}$ through L processing layers. This mapping depends on parameters (or weights) $W = W_1, W_2, \ldots, W_L$ and the preceding layer's output.

This work considers convolutional layers, where each layer consists of F filter weights $Q^f \in \mathbb{R}^{a \times b}$ for $f = 1, \ldots, F$, generating a feature map $Y^f \in \mathbb{R}^{n' \times m'}$ from an input matrix $X \in \mathbb{R}^{n \times m}$ based on the convolution operation:

$$Y^f_{(i,j)} = \sum_{k=0}^{a-1} \sum_{l=1}^{b-1} Q^f_{(a-k,b-l)} X_{(1+s(i-1)-k,1+s(j-1)-l)}, \quad (1)$$

where $s \geq 1$ represents the stride parameter, and the output dimensions are given by

$$n' = 1 + \left\lfloor \frac{n + a - 2}{s} \right\rfloor \quad (2)$$

and

$$m' = 1 + \left\lfloor \frac{m + b - 2}{s} \right\rfloor. \quad (3)$$

A CNN-based autoencoder is employed, as illustrated in Fig. 1. The convolutional layer, governed by (1), enables the transmitter to process sequences of symbols S, handling $k \times L$ bits in parallel. Each symbol in S is encoded as a one-hot vector $O_s \in \mathbb{R}^{2^k}$, where a single element is set to one while the rest remain zero.

To facilitate both linear and nonlinear block encoding of the input sequence, exponential linear unit (ELU) activation functions are utilized in the convolutional layers, transforming the one-hot input sequence S into a new representation $X = f(S)$ across n channel slots. This results in signal constellation points mapped into a $2n$-dimensional space. Each convolutional layer is followed by batch normalization to enhance network stability, employing 256 filters to optimize the representation of input symbols.

TABLE I
Autoencoder Layout

Block	Layer	Activation	Output Dim.
Encoder	Input		$L \times 2^k$
	Conv1D	ELU	$L \times 256$
	Conv1D	ELU	$L \times 256$
	Conv1D	LINEAR	$L \times 2n$
	Normalization		$L \times 2n$
Channel	Fading + Noise		$L \times 2n$
Decoder	Conv1D	ELU	$L \times 256$
	Conv1D	ELU	$L \times 256$
	Conv1D	SOFTMAX	$L \times 2^k$

Normalization layers enforce transmitter power constraints by mapping symbol representations into a $2n$-dimensional space, considering that each of the n channel slots consists of in-phase and quadrature (I/Q) components. The channel layer follows the conditional probability density function $p(Y|X)$ based on a κ-μ distribution, discussed further in the subsequent section. Additionally, additive white Gaussian noise (AWGN) with variance $\sigma^2 = (2RE_b/N_0)^{-1}$ is introduced, where $R = k/n$ represents the transmission rate, and E_b/N_0 denotes the signal-to-noise ratio (SNR).

The receiver adopts an architecture similar to the transmitter but omits the normalization layer. It reconstructs the received signal Y to classify each signal among 2^k possible candidates. Perfect CSI is assumed to be available and integrated into the receiver network alongside Y. A soft decision approach uses a softmax activation function, which outputs a probability vector over all possible input sequences S. The final transformation is denoted as $\hat{S} = g(Y)$, corresponding to the index of the highest-probability element in the output vector. Table I summarizes the autoencoder configuration used in this work.

The objective of this self-learning system is to determine the optimal set of parameters W^* that minimizes the loss function $J(W)$, given by

$$W^* = \arg\min_W J(W). \quad (4)$$

The optimization is performed using stochastic gradient descent (SGD), initialized with random weights $W = W_0$, and iteratively updated as follows:

$$W_{t+1} = W_t - \eta \nabla_w \tilde{J}(W_t), \quad (5)$$

where $\eta > 0$ is the learning rate, and ∇_w represents the gradient of the approximated binary cross-entropy (BCE) loss $\tilde{J}(W)$, computed for a randomly selected minibatch $N_t \subset 1, 2, \ldots, N$ of size N_t at each iteration:

$$\tilde{J}(W) = -\frac{1}{N_t} \sum_{i \in N_t} S_i \log(g(Y_i)). \quad (6)$$

The loss is optimized via backpropagation over the dataset of size N, facilitating improved performance of the autoencoder-based communication system.

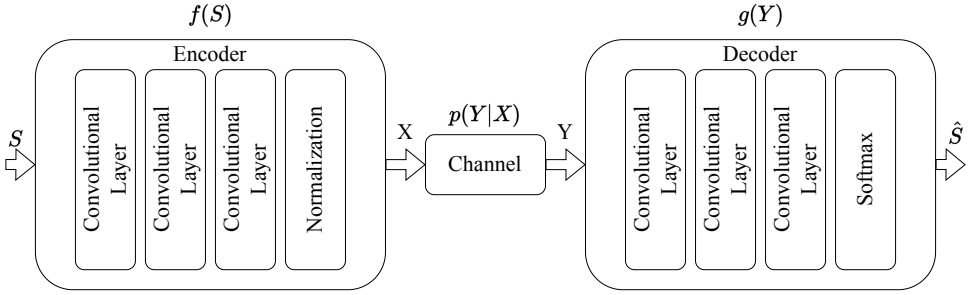

Fig. 1. End-to-End communication system as an autoencoder.

III. Channel Model

The κ-μ fading model represents a generalized statistical distribution that characterizes small-scale variations in fading signals under line-of-sight (LOS) and non-line-of-sight (NLOS) conditions. Unlike conventional models, the κ-μ distribution accounts for both multipath wave clusters and the non-linearity of the propagation environment. Several well-known fading models, such as the Exponential, Rayleigh, Nakagami-m, Gamma, and Weibull distributions, are special cases of the κ-μ distribution. The parameter κ describes the power ratio of dominant components to scattered waves, whereas μ represents the number of multipath clusters. Consequently, the signal envelope follows a nonlinear function based on the sum of multipath components, expressed as

$$r^2 = \sum_{i=1}^{n}(x_i + p_i)^2 + \sum_{i=1}^{n}(y_i + q_i)^2, \tag{7}$$

where x_i and y_i are independent Gaussian processes with expectations $E(x_i) = E(y_i) = 0$ and variances $E(x_i^2) = E(y_i^2) = \sigma^2$. Additionally, p_i and q_i denote the mean values of the in-phase and quadrature components of the multipath clusters.

Given a fading signal with envelope r and normalized envelope $\rho = r/\hat{r}$, where $\hat{r} = \sqrt{E(r^2)}$ represents the root-mean-square (RMS) value of r, the probability density function (PDF) of ρ is defined as [11, eqn.(1)]

$$p(\rho) = \frac{2\mu(1+\kappa)^{\frac{\mu+1}{2}}}{\kappa^{\frac{\mu-1}{2}}e^{\mu\kappa}}\rho^{\mu}e^{-\mu(1+\kappa)\rho^2}I_{\mu-1}\left(2\mu\sqrt{\kappa(1+\kappa)}\rho\right), \tag{8}$$

where $\kappa \geq 0$ is the ratio of the total power of dominant components to that of scattered waves, and $\mu \geq 0$ is given by

$$\mu = \frac{E^2(r^2)}{\mathrm{Var}(r^2)} \times \frac{1+2\kappa(1+\kappa)^2}{(1+\kappa)^2}. \tag{9}$$

Furthermore, the constraint $\frac{\mu(1+\kappa)^2}{1+2\kappa} \geq \frac{1}{2}$ must hold. Here, $I_v(.)$ denotes the modified Bessel function of the first kind of order v.

Several well-known fading models can be derived as special cases of the κ-μ distribution. The Weibull distribution is obtained by setting $\mu = 1$ and adjusting κ accordingly. The Rayleigh distribution emerges when $\mu = 1$ and $\kappa = 0$. The Nakagami-m distribution is a specific case of the κ-μ model where $\kappa = 0$, with m representing the multipath clusters.

A. BLER in κ-μ Fading Channels

To derive the BLER for flat κ-μ fading channels, we define the instantaneous SNR as $\gamma = R^2$, where R represents the fading envelope, the average SNR is given by: $\bar{\gamma} = \mathbb{E}[\gamma]$.

By applying standard transformation techniques for random variables from ρ, the probability density function (PDF) of γ is expressed as

$$f_\gamma(\gamma) = \frac{2\mu(1+\kappa)^{(\mu+1)/2}}{\Gamma(\kappa^{(\mu-1)/2}\exp(\mu\kappa))}\gamma^{\mu/2-1} \times e^{-\mu(1+\kappa)\gamma}I_{\mu-1}(2\mu\sqrt{\kappa(1+\kappa)\gamma}). \tag{10}$$

The unconditional error probability P_e is defined as

$$P_\mathrm{e} = \int_0^\infty p_\mathrm{e}(\gamma)f_\gamma(\gamma)d\gamma, \tag{11}$$

where $p_\mathrm{e}(\gamma)$ depends on the modulation scheme. For instance, in Coherent M-ary quadrature amplitude modulation (MQAM) modulation schemes, the error probability is approximated as

$$p_\mathrm{e}(\gamma) = Q\left(\sqrt{\frac{3\gamma\log_2 M}{M-1}}\right), \tag{12}$$

where $Q(.)$ represents the Q-function, defined as $Q(x) = \frac{1}{2\pi}\int_x^\infty \exp(-u^2/2)du$, and M is the modulation order. For binary phase shift keying (BPSK) and quadrature phase shift keying (QPSK) systems, the error probability can be approximated as

$$p_\mathrm{e}(\gamma) = Q(\sqrt{2\gamma}). \tag{13}$$

IV. Performance Analysis

This section presents a detailed evaluation of the CNN-based autoencoder's performance under κ-μ fading conditions, focusing on BLER results obtained from the simulation figures. The training dataset used to develop the CNN-based autoencoder consists of 16000 training messages and 80000 validation messages, each containing a block length of L symbols and each symbol conveying k information bits. The training SNR was set to $E_b/N_0 = 30$ dB to ensure robustness in high-SNR regimes. The training process utilized the Adam optimizer to facilitate rapid convergence, with a learning rate of $\eta = 0.001$, and mini-batches of size 64 were employed to ensure stable learning dynamics. The dataset was generated using independent and identically distributed (i.i.d) binary sequences drawn from a uniform distribution.

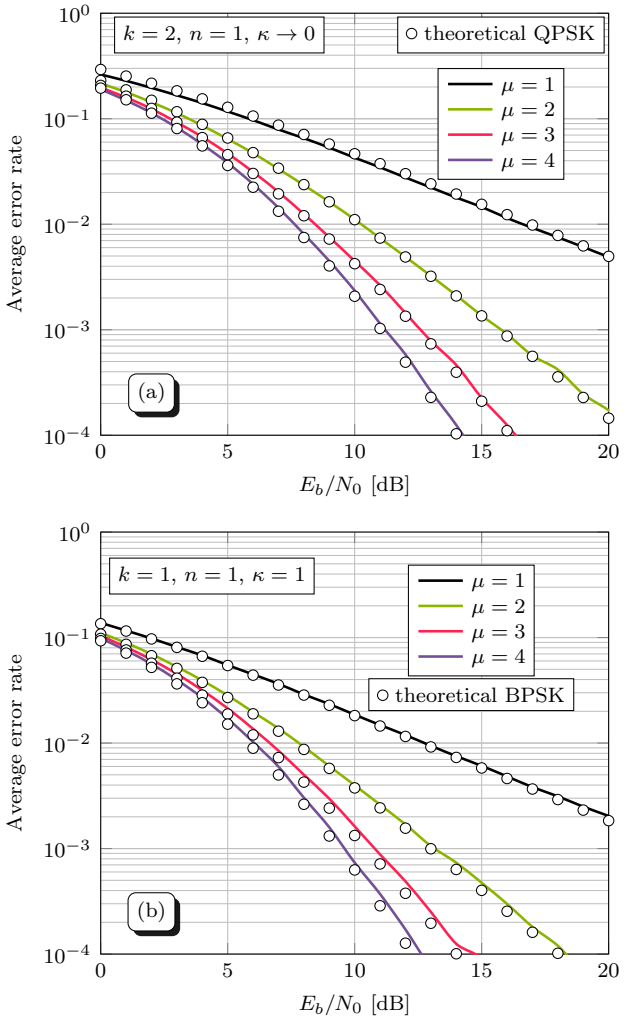

Fig. 2. Average error rate under the variation of parameter μ for fixed $n = 1$, (a) $k = 2$ and $\kappa \to 0$, and (b) $k = 1$ and $\kappa = 1$.

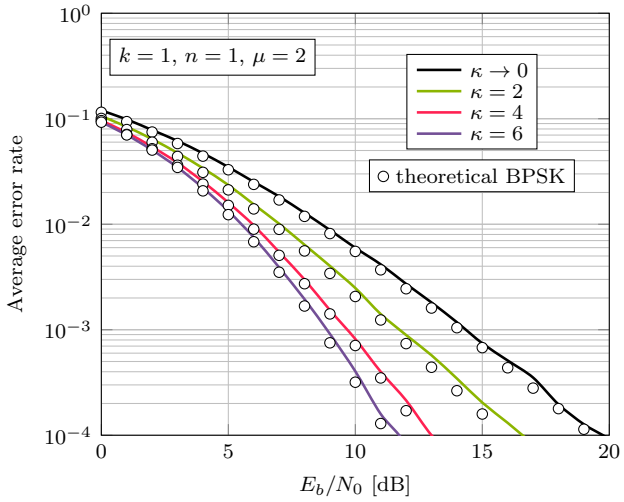

Fig. 3. Average error rate under the variation of parameter κ.

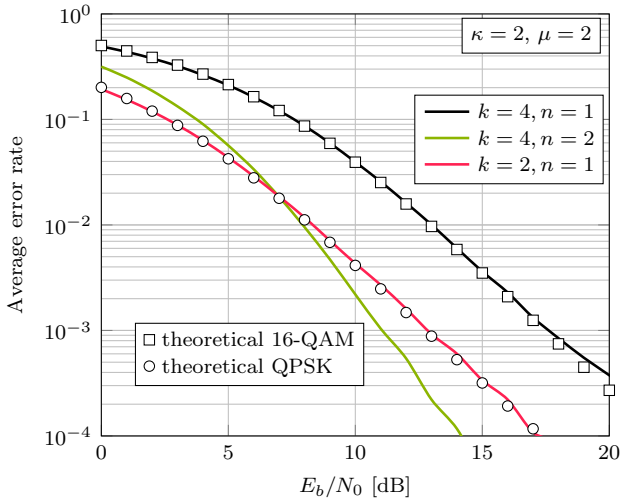

Fig. 4. Average error rate under the variation of parameter k.

Fig. 2(a) illustrates the impact of the multipath clustering parameter μ on BLER performance for different values of μ, with a fixed $k = 2$ and $n = 1$, under the condition where $\kappa \to 0$, representing a Nakagami-m fading scenario. Theoretical BLER curves for QPSK modulation are provided as a benchmark. As expected, increasing μ results in improved BLER performance, as larger values of μ correspond to less severe fading conditions. Fig. 2(b) presents results for a similar scenario but with $k = 1$, $n = 1$, and $\kappa = 1$. The theoretical BLER curve for BPSK modulation is included for comparison. The results indicate a similar trend to Fig. 2(a), where increasing μ leads to enhanced BLER performance. The CNN-based autoencoder exhibits robustness across varying fading conditions, adapting to different power distributions and matching the performance of the theoretical BLER.

Fig. 3 examines the effect of varying the power ratio parameter κ on the BLER performance while maintaining $\mu = 2$, $k = 1$, and $n = 1$. The theoretical BLER for BPSK modulation is included for reference. The results confirm that the fading conditions improve as κ increases, leading to lower BLER values. The CNN-based autoencoder is shown to match the theoretical BPSK BLER performance, suggesting that the system can learn optimal symbol mapping strategies for different power ratios without requiring explicit channel modeling.

Fig. 4 explores the impact of increasing the number of transmitted information bits k on the BLER. It compares different values of k and n while maintaining $\kappa = 2$ and $\mu = 2$. The theoretical BLER curves for 16-QAM and QPSK modulation schemes are also included for validation. The results highlight that increasing the number of bits per transmission results in a degradation in BLER, as expected. However, the CNN-based autoencoder successfully adapts to these conditions and maintains performance close to traditional modulation schemes, demonstrating its robustness in higher data rate scenarios.

Finally, Fig. 5 analyzes the learned constellation points for $R = 2$, showcasing the autoencoder's ability to self-organize its symbol mappings under κ-μ fading conditions. The plotted constellation diagram suggests that the autoencoder learns a

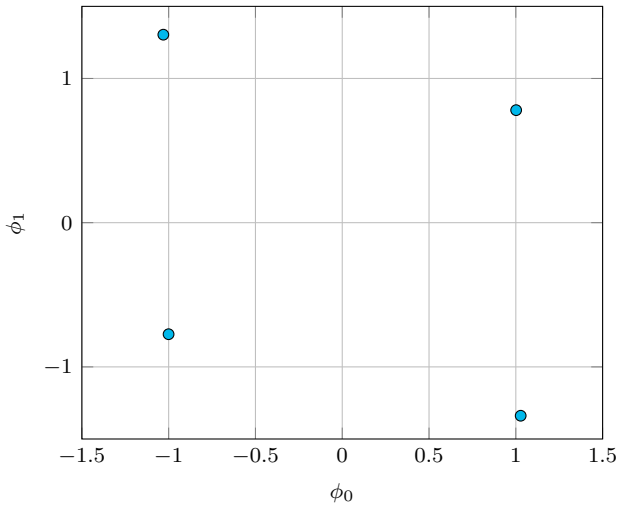

Fig. 5. Example of learned constellation.

QPSK-like structure with an arbitrary rotation, confirming that the system optimizes symbol placement to minimize decoding errors. This result further supports the adaptability of the CNN-based autoencoder in dynamic channel environments.

V. Conclusions

This paper investigated the BLER performance of a CNN-based autoencoder as an end-to-end communication system adapted to the generalized κ-μ fading model. The system was trained under various fading conditions and successfully learned optimal encoding and decoding strategies, achieving performance close to modulation schemes.

The results indicate that the CNN-based autoencoder can dynamically adapt to different multipath and power ratio parameters, demonstrating robustness under varying channel conditions. By learning optimal symbol mappings, the model matched the performance of conventional modulation schemes, such as QPSK and BPSK, across a range of SNR values. Moreover, the analysis of learned constellations highlighted the system's ability to optimize symbol placement, further validating its adaptability to complex fading environments.

One of the key challenges in designing practical wireless communication systems is ensuring a sufficient link margin to account for stochastic variations in SNR. The proposed framework offers a flexible and adaptive approach that can dynamically adjust to real-world channel conditions, potentially reducing the complexity of system planning and resource allocation. The ability of DL-based systems to generalize over different block lengths, code rates, and channel uses further supports their viability for next-generation wireless networks.

Acknowledgments

This work was partially funded by CNPq (Grant Nos. 302085/2025-4 and 306199/2025-4), by Minas Gerais Research Foundation (FAPEMIG) (Grant Nos. PPE-00124-23, APQ-04523-23, APQ-05305-23, and APQ-03162-24), by the Brasil 6G project (1245.010604/2020-14), supported by RNP and MCTI, and by the projects XGM-AFCCT-2024-2-5-1 and XGM-AFCCT-2024-9-1-1 supported by xGMobile – EMBRAPII-Inatel Competence Center on 5G and 6G Networks, with financial resources from the PPI IoT/Manufatura 4.0 from MCTI grant number 052/2023, signed with EMBRAPII.

References

[1] K. Nakashima, S. Kamiya, K. Ohtsu, K. Yamamoto, T. Nishio, and M. Morikura, "Deep reinforcement learning-based channel allocation for wireless lans with graph convolutional networks," 2019. [Online]. Available: https://arxiv.org/abs/1905.07144

[2] S. R. Doha and A. Abdelhadi, "Deep learning in wireless communication receiver: A survey," 2025. [Online]. Available: https://arxiv.org/abs/2501.17184

[3] T. O'Shea and J. Hoydis, "An introduction to deep learning for the physical layer," *IEEE Transactions on Cognitive Communications and Networking*, vol. 3, no. 4, pp. 563–575, 2017.

[4] H.-Y. Chen, M.-H. Wu, T.-W. Yang, C.-W. Huang, and C.-F. Chou, "Attention-aided autoencoder-based channel prediction for intelligent reflecting surface-assisted millimeter-wave communications," *IEEE Transactions on Green Communications and Networking*, vol. 7, no. 4, pp. 1906–1919, 2023.

[5] Z. Huang, D. He, J. Chen, Z. Wang, and S. Chen, "Autoencoder with fitting network for terahertz wireless communications: A deep learning approach," *China Communications*, vol. 19, no. 3, pp. 172–180, 2022.

[6] H.-P. Yin, X.-H. Zhao, J.-L. Yao, and H.-P. Ren, "Deep-learning-based channel estimation for chaotic wireless communication," *IEEE Wireless Communications Letters*, vol. 13, no. 1, pp. 143–147, 2024.

[7] S. Dörner, S. Cammerer, J. Hoydis, and S. t. Brink, "Deep learning based communication over the air," *IEEE Journal of Selected Topics in Signal Processing*, vol. 12, no. 1, pp. 132–143, 2018.

[8] H. Safi, I. Tavakkolnia, and H. Haas, "Deep learning based end-to-end optical wireless communication systems with autoencoders," *IEEE Communications Letters*, vol. 28, no. 6, pp. 1342–1346, 2024.

[9] S. Gomes and M. Yacoub, "CNN-based learning system in a generalized fading environment," in *XXXVIII Simpósio Brasileiro de Telecomunicações e Processamento de Sinais*, 2020.

[10] P. M. R. Pereira, T. A. M. de Bairros, R. A. A. de Souza, and M. D. Yacoub, "Mobility, path loss, and composite fading: Performance of a conventional and of a non-conventional system with a robust autoencoder," *IEEE Transactions on Vehicular Technology*, vol. 72, no. 12, pp. 16 725–16 730, 2023.

[11] M. D. Yacoub, "The κ-μ distribution and the η-μ distribution," *IEEE Antennas Propag. Mag.*, vol. 49, no. 1, pp. 68–81, 2007.